Influence of Magma Supply on Galápagos Spreading Center Magmatic & Eruptive Processes

A. Colman[1], J.M. Sinton[1], S.M. White[2]

[1]University of Hawai'i, [2]University of South Carolina

SCHOOL OF OCEAN AND EARTH SCIENCE AND TECHNOLOGY
UNIVERSITY OF HAWAI'I AT MĀNOA

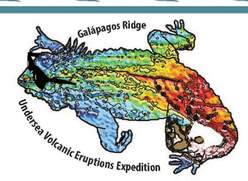

Galápagos Spreading Center

Regional Trends

A significant increase in the rate of magma supply to the crust with proximity to the Galápagos hotspot along the Galápagos Spreading Center (GSC) makes this area ideal for studying the effects of variable magma supply on mid-ocean ridge (MOR) magmatic and eruptive processes. With increasing proximity to the hotspot, the spreading axis and axial magma chamber become increasingly shallow, the crust thickens, and the axial morphology changes from an axial valley to an axial rise. The plume influence is detectable in lava compositions along the ridge as well, with increasing enrichments in incompatible elements near the hotspot. The maximum plume influence on the ridge is reached near 91°W. We have identified lava flow fields from individual eruptive episodes in two ~20 km-long detailed study areas (DSA's) along the spreading axis of the GSC, one at 95W and the other 330 km to the east at 92W; over this interval the rate of magma supply increases by 40%, while the spreading rate remains nearly constant (52-56 mm/yr).

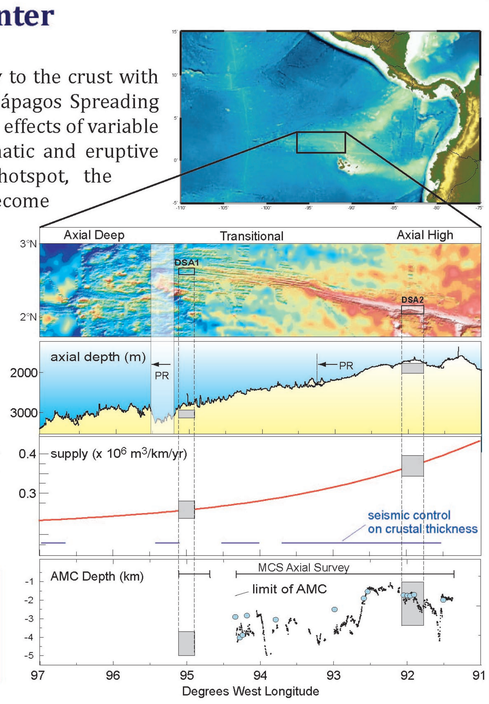

At right: DSA locations along western GSC with respect to regional trends in (from top to bottom): axial morphology; seafloor roughness and axial depth; magma supply; and AMC depth and crustal thickness. Figure modified from Detrick et al. (2002).

Submarine Geologic Mapping

At each DSA, high-resolution bathymetry data (~2 m spatial resolution) were collected to augment the existing multibeam coverage. In addition, rock samples were taken and observations of the geologic relationships and sediment cover on the seafloor were recorded during 26 Alvin dives and 16 TowCam deployments. These observations, inferences from the bathymetric maps, and microprobe analyses of glass from the rock samples were synthesized to create detailed geologic maps for each area.

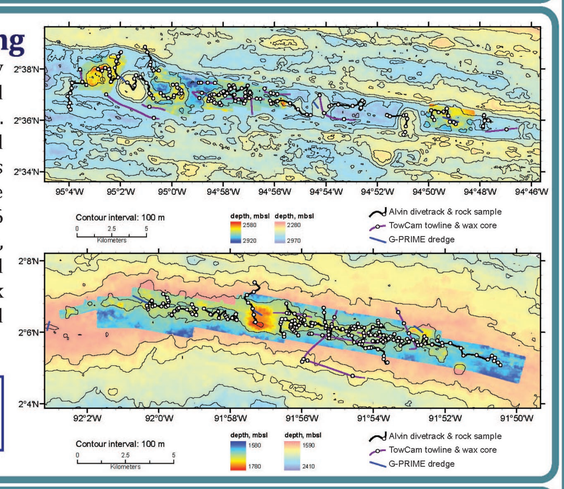

At right: Datasets used in the preparation of the geologic maps. Brighter colors are areas mapped at high resolution using AUV Sentry. See legend for symbols.

Geologic Maps

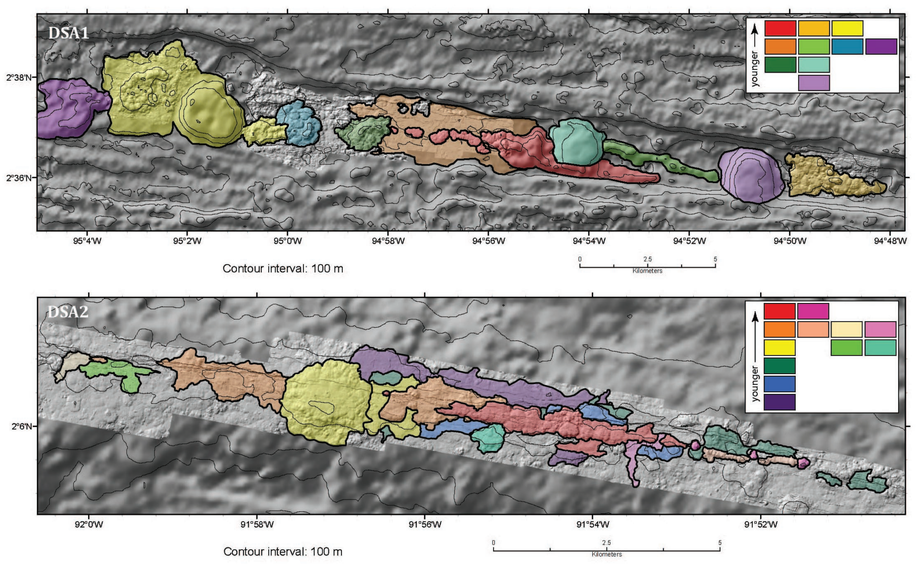

Above: Geologic maps prepared using the datasets described above. Relative age relationships are displayed in boxes in upper righthand corner of each map, with the youngest units at the top of each column; colors correspond to those used in the maps.

Lava Morphology: a Proxy for Eruption Rate

Submarine lava morphologies can be classified as pillows, lobate flows, folded sheets, or jumbled sheets. Analog experiments have shown that lava morphology is controlled by the relative rates of lava cooling and flow. Within a given environment, where cooling rates are unlikely to vary widely, flow morphology is largely controlled by the lava effusion rate, viscosity, and temperature, and has been used as a proxy for eruption rate (Gregg et al., 1996); with increasing eruption rate, pillows, lobate flows, and sheet flows are produced successively.

Differences in lava morphology occurrence

Observations of flow morphologies within our study areas indicate that pillows are more common at low magma supply than at high magma supply. At low magma supply, the flanks of the prominent mounds and seamounts within the inner axial graben are composed almost entirely of pillows, while lobate flows are somewhat more common on the mounds' relatively flat summit regions. One eruptive unit near the center of the study area filled the floor of the inner axial graben with lobate and sheet flows, but it is anomalous. At high magma supply, pillows are still the most common lava morphology, but both lobate and sheet flows are more abundant, forming channels, low-relief mounds, and partially collapsed lava lakes. These observations suggest that on average, eruption rates are higher at high magma supply, although more work is needed to account for the influence of viscosity on the observed morphologies.

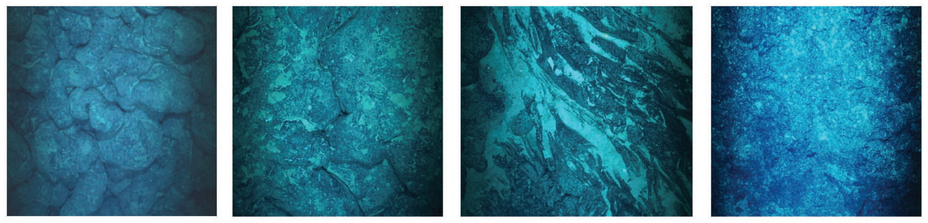

Above: Observed lava flow morphologies. From left to right, pillows; lobate flows; folded sheets; jumbled sheets.

Morphological differences reflect eruptive processes

Eruptive edifices

At high magma supply, eruptive units are generally more elongated; the majority of eruptive units are either narrow pillow ridges oriented parallel or sub-parallel to the spreading axis, or chains of eruptive vents feeding lower-relief lobate and sheet flows. Locally, elongate units are discontinuous along their lengths, forming discrete pillow mounds, but more commonly, they form continuous ridges. At low magma supply, eruptions more frequently produce roughly equidimensional clusters of steep-sided pillow mounds. The predominance of point source constructs over line source constructs at low magma supply may be a further indication of lower average eruption rates. It is unclear at present whether the difference in the dominant eruptive style is primarily controlled by differences in the magma chamber depth, lava viscosity, regional tectonic setting, or some other factor.

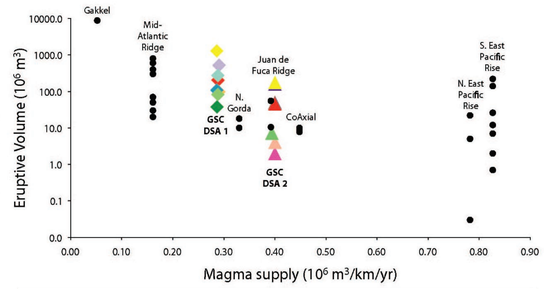

Above: Relationship between magma supply and eruptive volume for global set of mapped MOR eruptive units. Symbol colors correspond to GSC eruptive units in geologic maps at left. Diamonds: DSA1; Triangles: DSA2. Black circles represent other mapped MOR eruptions, from compilation in Sinton et al. (2001).

Eruptive volumes

The volumes of individual eruptive units were determined by calculating the volume above a basal contour for mounded units, and by multiplying an assumed thickness by the mapped area for planar units. These calculated eruptive volumes range over several orders of magnitude at each study area, but on average, eruptive volumes are larger at low magma supply. This is consistent with the general trend exhibited by the global set of mapped MOR eruptive units, and suggests that eruptions occur more frequently at high magma supply.

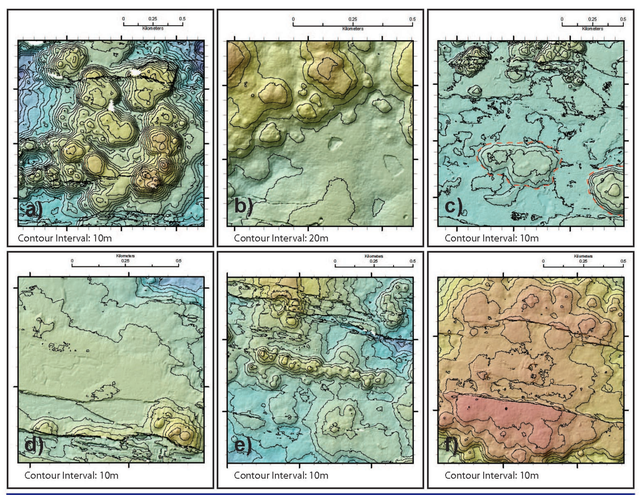

Above: Eruptive edifice morphology. **a-c**, DSA1. **d-f**, DSA2. **a)** Cluster of steep-sided pillow mounds with summit plateaus. **b)** Low-lying, low-relief lava shields with collapsed summit craters at the base of a larger eruptive edifice. **c)** Lava channels; tumuli; and low-lying, low-relief lobate flows. Source of eruption is fissure that crosscuts preexisting mounds to the north. Flows are partially buried by a later fissure eruption that produced a chain of pillow mounds (within dashed red lines). **d)** Low-relief partially collapsed lobate flows build broad lava plain sloping down away from spreading center. **e)** Chain of steep-sided, fissure-fed pillow mounds near axis of spreading. **f)** Broad summit region of most prominent mound along spreading axis at DSA2. Note presence of several tumuli within axial graben.

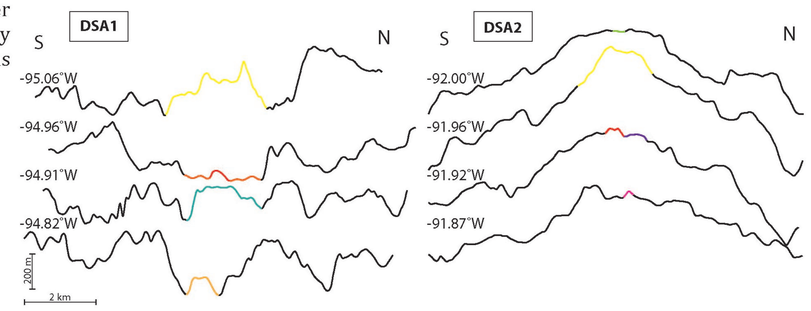

Above: Axial morphology: profiles along four roughly S-N transects across the spreading center at each study area. Colored portions of profiles correspond to eruptive units in geologic maps at left; black portions of profiles are unmapped seafloor. Note contrasts in fault offsets and eruptive edifice heights contributing to overall smoothness of seafloor at each study area.

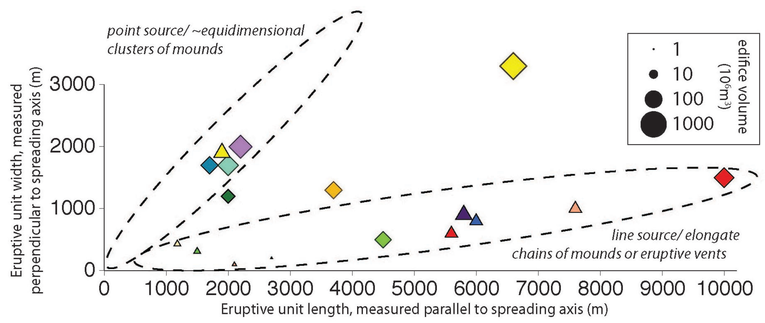

Above: Map-view dimensions of mapped GSC eruptive units. Symbol colors correspond to eruptive units in geologic maps at left. Symbol size is proportional to log of eruptive volume. Diamonds: DSA1; Triangles: DSA2.

Compositional differences yield insight into magmatic processes

Extent of differentiation

At low magma supply, compositional variation is restricted to relatively unfractionated compositions (6.2-9.1 wt. % MgO), while at high magma supply, compositions range to much greater extents of fractionation (2.7-8.0 wt. % MgO). This observation is consistent with the seismically determined depth of the axial magma chamber at each study area. An AMC residing at shallower depths within the crust (as at DSA2) could be expected to experience more efficient cooling, promoting crystallization of the resident magma, and resulting in more differentiated erupted lavas. The wide range in MgO content of sampled lavas within a ridge segment could reflect temporal variability in the resident magma, or the presence of multiple discrete magma reservoirs; better constraints on the ages of the mapped units will help to differentiate between these possibilities.

Enrichment in incompatible elements

Lavas are significantly more enriched in the most incompatible elements in the high magma supply study area than in the low magma supply study area (0.26-0.34 K/Ti; 0.09-0.12 Nb/Zr vs. 0.06-0.15 K/Ti; 0.05-0.07 Nb/Zr). K/Ti ratios within individual eruptive units are also more variable at higher magma supply. Previous studies have shown that the greater degrees of enrichment in incompatible elements near the hotspot could be produced by low degrees of melting over an expanded hydrous melting zone (Cushman et al., 2004; Ingle et al., 2010).

Lava crystallinity

At low magma supply, samples range from dominantly plagioclase-phyric to dominantly olivine-phyric, and crystallinity (estimated in hand sample) ranges from nearly aphyric to 20%. Disequilibrium textures are common within certain eruptive units, suggesting that some intra-flow chemical variation is mixing-related. At high magma supply, samples are overwhelmingly phenocryst-free, although some samples contain large numbers of microphenocrysts. The prevalence of aphyric lavas at DSA2 suggests that eruptions are commonly fed by melt-rich magma reservoirs, which is consistent with the strong reflector in the seismic data.

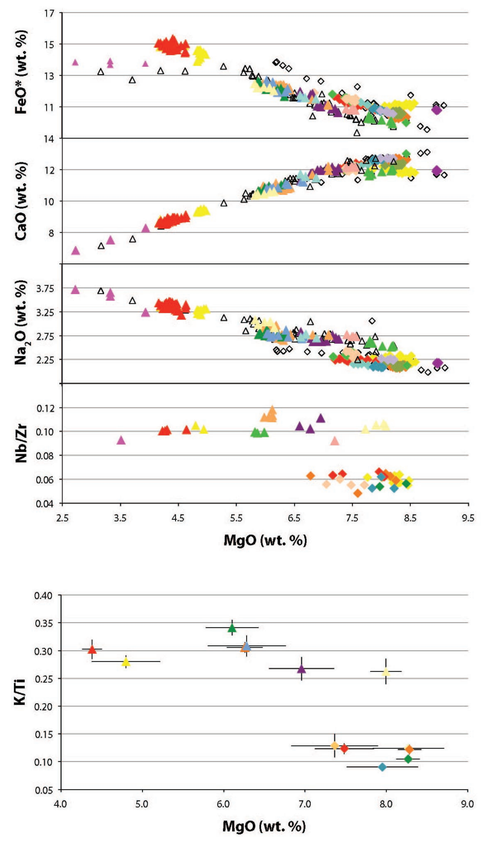

Upper right: Chemical variation diagrams for selected major elements and Nb/Zr. Major element compositions were determined by glass microprobe analysis; trace element compositions were determined by whole rock x-ray fluorescence analysis. DSA2 is elevated in Na_2O, TiO_2, K_2O, and P_2O_5, and depleted in FeO* at a given MgO content, relative to DSA1. Symbol colors correspond to eruptive units in geologic maps at left. Hollow symbols have not been assigned to an eruptive unit. Diamonds: DSA1; Triangles: DSA2.
Lower right: Measures of two types of intra-flow compositional heterogeneity. MgO content is controlled largely by the amount of fractionation that has occured; K/Ti is largely unaffected by fractionation until Fe/Ti oxides begin to crystallize, and therefore is a good measure of parental magma heterogeneity (whether source- or degree of melting-related). Symbols represent eruptive unit means for units with at least 7 samples, with colors corresponding to eruptive units in geologic maps at left. Diamonds: DSA1; Triangles: DSA2. Error bars are standard deviation (2σ) about the mean.

	Melt Generation	Magma Reservoirs	Eruptive Style
Low Magma Supply	Smaller melt zone Higher average degree melting	Deep (~4 km) Crystal-rich Intermittent	Lower effusion-rate Larger volume Point sources (seamounts)
High Magma Supply	Additional zone of deep hydrous melting Lower average degree melting	Shallow (~1.5 km) Melt-rich Quasi-steady-state	Higher effusion rate Smaller volume Line sources (fissures)

References:

Cushman, B., Sinton, J., Ito, G, and Dixon, J. E., 2004, Glass composition, plume-ridge interaction, and hydrous melting along the Galápagos Spreading Center, 90.5°W to 98°W: Geochemistry Geophysics Geosystems, v. 5, 30 p.

Detrick, R. S., Sinton, J. M., Ito, G., Canales, J. P., Behn, M., Blacic, T., Cushman, B., Dixon, J. E., Graham, D. W., and Mahoney, J. J., 2002, Correlated geophysical, geochemical, and volcanological manifestations of plume-ridge interaction along the Galápagos Spreading Center: Geochemistry Geophysics Geosystems, v. 3, 14 p.

Gregg, T. K. P. and Fink, J. H., 1995, Quantification of submarine lava-flow morphology through analog experiments: Geology, v. 23, p. 73-76.

Ingle, S., Ito, G., Mahoney, J.J., Chazey, W., Sinton, J., Rotella, M., Christie, D., 2010, Mechanisms of geochemical and geophysical variations along the western Galápagos Spreading Center: Geochemistry Geophysics Geosystems, v. 11, 30 p.

Sinton, J., Bergmanis, E., Rubin, K., Batiza, R., Gregg, T. K., P., Grönvold, Macdonald, K. C., and White, S. M., 2001, Volcanic eruptions on mid-ocean ridges: New evidence from the superfast spreading East Pacific Rise, 17°-19°S: Journal of Geophysical Research, v. 107, 20p.